Loss of Rotor Isotropy As a Blade Damage Indicator for Wind Turbine Structure Health Monitoring Systems

Dmitri Tcherniak

7th European Workshop on Structural Health Monitoring
July 8-11, 2014. La Cité, Nantes, France

LOSS OF ROTOR ISOTROPY AS A BLADE DAMAGE INDICATOR FOR WIND TURBINE STRUCTURE HEALTH MONITORING SYSTEMS

Dmitri Tcherniak

Brüel & Kjær SVM, Skodsborgvej 307, Nærum 2850, Denmark
dmitri.tcherniak@bksv.com

ABSTRACT

Modal-based damage features utilizing asymmetry of the rotor whirling mode shapes arising from rotor anisotropy are examined by Floquet analysis, and output-only modal analysis is applied to simulated vibrations of a rotating rotor.

KEYWORDS : *wind turbine blade, rotor anisotropy, Floquet analysis, OMA*

INTRODUCTION

Blades of modern wind turbines are complex high-tech structures, and their cost constitutes a significant part of the entire wind turbine cost. While operating, the blades are heavily loaded and exposed to harsh weather conditions, especially for off-shore wind turbines. If damage to the blades develops to a critical level it may cause catastrophic consequences. If the damage leads to partial or complete loss of structural integrity, the repair is extremely costly, or may even be impossible. This calls for automatic blade health monitoring systems, which are able to automatically detect and report the damage, follow up on damage development and guide the blade Operational and Maintenance program in general.

The approach presented in this paper is not new: we apply operational modal analysis (OMA) to vibration data measured on an operating wind turbine [1]. The changes in the obtained modal parameters are used to detect and localise the damage. However, in this study, we use a pragmatic view: we are looking for the blade damage features sufficiently *sensitive*, and these features should be *observable* in a real-life situation. The following two examples demonstrate the opposite: It is known that damage changes natural frequencies of the structure. However, many conclude [2] that these changes are not sensitive to the damage, i.e., the damage must grow an extreme amount to change the natural frequencies significantly enough to be detectable. It is also known that the mode shapes of flapwise blade modes can be used to localise blade damage [3]. However, it was shown [4, 5] that for operating wind turbines, the flapwise modes are not observable with the accuracy level sufficient for damage localisation.

We also admit that OMA, though being a valuable tool for big structures, is not perfectly suited for operating wind turbines. The acting aerodynamic loads do not satisfy OMA assumptions [6] and, in general, an operating wind turbine cannot be modelled as a time-invariant system. A linear time-periodic (LTP) system is a better model for an operating wind turbine; for modal decomposition of such systems, a number of dedicated methods have been developed, e.g., [7, 8]. However, here we also use a pragmatic approach: the goal is not to perform a perfect modal identification, but rather define the dynamic features which can be used for confident damage detection.

This explains the selection of damage features for this study: From practical experience [5], it was noticed that the magnitude and phases between the blades for *whirling modes* demonstrate high level of sensitivity to blade damage. Also from experience [4, 5], it is known that the *edgewise whirling* modes can be identified with a high level of confidence. Based on these considerations, it was decided to examine how a slight rotor anisotropy due to damage influences the mode shape of the in-plane whirling modes, with the focus on phase and magnitude of the blade motion.

This paper suggests the following investigation strategy: Section 1 sets up a lumped-mass model of a three-bladed rotor, simple but sufficient for catching the first in-plane rotor modes. The equations

of motion are derived, and modal decomposition based on Floquet analysis is performed. This analytical approach provides almost exact modal decomposition and helps understanding of the dynamics of the undamaged (isotropic) and damaged (anisotropic) rotor.

Section 2 is based on a simulated experiment of the lumped-mass model: it assumes the equations of motion are not known; the dynamic of the simplified system loaded by random forces is simulated, and the resulting time histories are input to OMA. The results will prove if OMA is capable of confidently providing the damage features, now from the experimental viewpoint.

1 SIMPLIFIED ROTOR MODEL

A simple six degree-of-freedom (DOF) system (Figure 1) models a rotating rotor and the supporting tower/nacelle structures. Each blade is modelled as two beams with lengths a and b, connected by a linear angular spring with stiffness k_j, j=1...3, where j is the blade index. The blades are evenly distributed over the rotor, the blades' azimuth angles are: $\psi_j(t) = \psi(t) + 2/3\,\pi(j-1)$. Lumped masses m_j are attached to the ends of the outer beams. The rotor rotates with the angular speed Ω about point C attached to the mass m_N, the latter models the nacelle. The mass is supported by two springs with stiffnesses k_H and k_V, which model the tower. The drivetrain has a moment of inertia I_D and stiffness k_D. A similar lumped parameter system is considered in [10], however, there the focus was on the out-of-plane rotor motion.

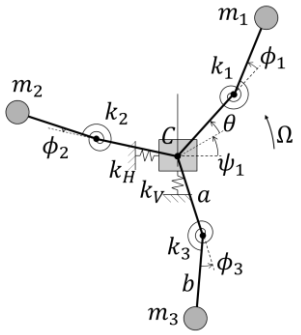

Figure 1: Simplified rotor system

The system is described by six coordinates: x_C and y_C are coordinates of point C, deflection of each blade from a straight line is described by angle ϕ_j, and θ is the drivetrain angular vibrations.

Equations of motion (EoM) are derived using the Lagrange method. The linearized EoM can be written as:

$$\mathbf{M}(t)\ddot{\mathbf{y}}(t) + \mathbf{G}(t)\dot{\mathbf{y}}(t) + \mathbf{K}(t)\mathbf{y}(t) = \mathbf{0}, \tag{1}$$

where:$\mathbf{M}(t)$, $\mathbf{G}(t)$ and $\mathbf{K}(t)$ are mass, gyroscopic and stiffness matrices. The matrices depend on the rotor azimuth $\psi(t)$; for constant rotor speed Ω, $\psi(t) = \Omega t + \psi_0$, the matrices are periodic with period $T = 2\pi/\Omega$: $\mathbf{M}(t) = \mathbf{M}(t+T)$, $\mathbf{G}(t) = \mathbf{G}(t+T)$, $\mathbf{K}(t) = \mathbf{K}(t+T)$. The vector $\mathbf{y}(t) = \{x_C(t), y_C(t), \phi_1(t), \phi_2(t), \phi_3(t), \theta(t)\}^T$ describes the physical DOFs of the system measured from the equilibrium position.

The *Coleman* (also known as *multiblade coordinate* or *MBC*) *transformation* converts the blade DOFs $\phi_j(t)$ to multiblade coordinates [9]:

$$a_0(t) = \tfrac{1}{3}\sum_{j=1}^{3}\varphi_j(t); \quad a_1(t) = \tfrac{2}{3}\sum_{j=1}^{3}\varphi_j(t)\cos(\psi_j(t)); \quad b_1(t) = \tfrac{2}{3}\sum_{j=1}^{3}\varphi_j(t)\sin(\psi_j(t)). \tag{2}$$

The Coleman transformation converts only blade DOFs, keeping the other DOFs unchanged. In matrix form the transformation can be written as:

$$\mathbf{y}(t) = \mathbf{D}(t)\,\mathbf{w}(t), \tag{3}$$

where: $\mathbf{w}(t) = \{x_C(t), y_C(t), a_0(t), a_1(t), b_1(t), \theta(t)\}^T$ is the vector of multiblade coordinates. The matrix $\mathbf{D}$ can be easily derived from (2) or found in e.g., [9]. It has the following properties [9]: $\mathbf{D}(t)^{-1} = \boldsymbol{\Gamma}\mathbf{D}(t)$, $\dot{\mathbf{D}}(t) = \mathbf{D}(t)\mathbf{R}$ and $\ddot{\mathbf{D}}(t) = \mathbf{D}(t)\mathbf{R}^2$ where $\boldsymbol{\Gamma}$ and $\mathbf{R}$ are time invariant matrices. Applying the transformation to (1), using the above-mentioned properties and pre-multiplying by $\mathbf{D}(t)^{-1}$ yield the equation of motion in multiblade coordinates:

$$\mathbf{M}_D(t)\ddot{\mathbf{w}}(t) + \big(2\mathbf{M}_D(t)\mathbf{R} + \mathbf{G}_D(t)\big)\dot{\mathbf{w}}(t) + \big(\mathbf{M}_D(t)\mathbf{R}^2 + \mathbf{G}_D(t)\mathbf{R} + \mathbf{K}_D(t)\big)\mathbf{w}(t) = \mathbf{0}, \quad (4)$$

where: $\mathbf{M}_D(t) = \boldsymbol{\Gamma}\mathbf{D}(t)^T\mathbf{M}(t)\mathbf{D}(t)$, $\mathbf{G}_D(t) = \boldsymbol{\Gamma}\mathbf{D}(t)^T\mathbf{G}(t)\mathbf{D}(t)$ and $\mathbf{K}_D(t) = \boldsymbol{\Gamma}\mathbf{D}(t)^T\mathbf{K}(t)\mathbf{D}(t)$. The important property of the Coleman transformation is that the matrices $\mathbf{M}_D(t)$ and $\mathbf{G}_D(t)$ *are time-invariant for isotropic rotors*: $m_1 = m_2 = m_3 = m$ and $k_1 = k_2 = k_3 = k$. For an isotropic rotor, $\mathbf{K}_D(t)$ is time-periodic with period $T/3$ due to the gravity.

For isotropic rotors, when the influence of gravity can be neglected, the Coleman transformation converts time-periodic EoM (1) into the time-invariant one. This allows application of conventional modal decomposition based on eigenvalue analysis of EoM (4). The results obtained by this approach lead to understanding of the collective and whirling components of the modes [9, 11].

In this study a deviation from the rotor isotropy is in focus, and the eigenvalue analysis cannot be applied. Still, since the considered deviations are assumed to be small, the results of the eigenvalue analysis of (4) might be useful as a starting point and the baseline for comparison.

Let's consider the rotor becoming slightly anisotropic, either due to damage, which causes some reduction of the stiffness of one of the blades, or by ice formation which causes a difference between the blade masses. In this situation, EoM (4) will have time-periodic coefficient matrices.

To obtain a solution to time-periodic EoM, several techniques could be employed. In his PhD thesis, Skjoldan describes and compares several methods (Table 3.1 in [12]), but in this study, classical Floquet analysis was chosen as the most appropriate[1].

The first order form of (1):

$$\dot{\mathbf{x}}(t) = \widetilde{\mathbf{A}}(t)\mathbf{x}(t), \quad (5)$$

where: $\mathbf{x}(t) = \{\dot{\mathbf{y}}(t)^T, \mathbf{y}(t)^T\}^T$ is the state vector (in multiblade coordinates) and $\widetilde{\mathbf{A}}(t) = \widetilde{\mathbf{A}}(t+T)$ is the periodic system matrix, the size of which is 12×12:

$$\widetilde{\mathbf{A}}(t) = \begin{pmatrix} -\mathbf{M}(t)^{-1}\mathbf{G}(t) & -\mathbf{M}(t)^{-1}\mathbf{K}(t) \\ \mathbf{I}_{6\times6} & \mathbf{0}_{6\times6} \end{pmatrix}. \quad (6)$$

Extending Coleman transformation to the first order form:

$$\mathbf{x}(t) = \mathbf{B}(t)\,\mathbf{z}(t), \quad (7)$$

one arrives at the first order equation in multiblade coordinates:

$$\dot{\mathbf{z}}(t) = \mathbf{A}(t)\mathbf{z}(t). \quad (8)$$

Following [13], the analysis is performed in a number of steps:

1. The *fundamental matrix* of the system is built: Equation (8) is numerically integrated for 12 linearly independent initial conditions. Denoting the solution for the j^{th} initial condition at time t as $\boldsymbol{\varphi}_j(t)$, the fundamental matrix is written as:
$$\boldsymbol{\Phi}(t) = [\boldsymbol{\varphi}_1(t) \quad \dots \quad \boldsymbol{\varphi}_{12}(t)], \quad (9)$$
where: $\boldsymbol{\Phi}(0) = \mathbf{I}$.
2. Then the *monodromy matrix* is computed as:
$$\mathbf{C} = \boldsymbol{\Phi}(0)^{-1}\boldsymbol{\Phi}(T) = \boldsymbol{\Phi}(T); \quad (10)$$
3. As *Lyapunov-Floquet transformation* transforms the time-periodic system (8) into a time-invariant one, we can compute its system matrix $\mathbf{R}$ as:
$$\mathbf{R} = \frac{1}{T}\ln(\mathbf{C}); \quad (11)$$
4. Eigenvalue decomposition of matrix $\mathbf{R}$ is performed:

[1] With insignificant changes, this paper uses the notations and follows derivation given in [13], where more details are provided.

$$\mathbf{R} = \mathbf{V}\boldsymbol{\Lambda}\mathbf{V}^{-1}, \tag{12}$$

where the columns of $\mathbf{V}$ are the eigenvectors $\mathbf{v}_j$, and the diagonal elements of $\boldsymbol{\Lambda}$ are the eigenvalues $\lambda_j = \sigma_j + \mathrm{i}\omega_j$, the real part is the damping and the imaginary part is the frequency. Actually, the same eigenvalues can be obtained as:

$$\lambda_j = \ln(\rho_j)/T, \tag{13}$$

where ρ_j are the eigenvalues of the monodromy matrix $\mathbf{C}$.

5. The *periodic mode shape* of the system (8) in the multiblade coordinates, is:

$$\mathbf{r}_j(t) = \boldsymbol{\Phi}(t)\mathbf{v}_j e^{-\lambda_j t}, \tag{14}$$

6. and in the blade coordinates is:

$$\mathbf{u}_j(t) = \mathbf{B}(t)\mathbf{r}_j(t) = \mathbf{B}(t)\boldsymbol{\Phi}(t)\mathbf{v}_j e^{-\lambda_j t}. \tag{15}$$

7. Since the logarithm in (13) is complex, any $\lambda_j = \sigma_j + \mathrm{i}(\omega_j \pm n\Omega), n \in \mathbb{Z}$ are also eigenvalues of $\mathbf{R}$. Similar to the principal value of a complex logarithm, the principal frequency is defined as

$$\omega_{\mathrm{p}j} = \omega_j - n_j\Omega, \;\; n_j\colon \omega_{\mathrm{p}j} \in \,]-\Omega/2; \Omega/2] \tag{16}$$

and the principal eigenvalue as $\lambda_{\mathrm{p}j} = \sigma_j + \mathrm{i}\omega_{\mathrm{p}j}$.

8. The j^{th} periodic mode shape (14) computed for the principal eigenvalue $\lambda_{\mathrm{p}j}$ is expanded to the Fourier series, and the most dominant Fourier component is identified, and its frequency is $n_{0j}\Omega$. For isotropic rotor, in the absence of gravity, the frequencies $\omega_{\mathrm{p}j} + n_{0j}\Omega$ coincide with the eigenfrequencies of the time-invariant system (4).
9. Finally, the periodic mode shape in blade coordinates (15) is also expanded to the Fourier series. The dominating Fourier components will be concentrated around the frequency $\omega_{\mathrm{p}j} + n_{0j}\Omega$; the behaviour of these components for different degrees of anisotropy are examined in the next section.

2 EXAMINATION OF THE MODAL DYNAMIC

For examination of the rotor modal behaviour, the following parameters were chosen: $m_N = 446\,10^3\ kg$, $m_1 = m_2 = m_3 = 41.7\,10^3\ kg$, $k_1 = k_2 = k_3 = 2.006\,10^8\ N\cdot m$, $k_D = 10^8\ N\cdot m$, $k_H = 2.6\,10^6\ N/m$, $k_V = 5.2\,10^8\ N/m$, $I_D = 2.6\,10^7\ kg\cdot m^2$, $a = b = 13.1\ m$, $\Omega = 2\pi\ 0.16\ rad/s$. These parameters approximate to the parameters of a generic 10 MW wind turbine model. A proportional damping term was introduced to (1): $(\alpha\,\mathbf{M}(t) + \beta\,\mathbf{K}(t))\dot{\mathbf{y}}(t)$; $\alpha = 0.05, \beta = 0.003$ were chosen for the examination.

After Coleman transformation, in the absence of gravity, equation (4) is time-invariant, and can be readily analysed using conventional eigenvalue analysis. Six modes are obtained and identified as vertical and horizontal motion of the nacelle mass, drivetrain mode and three rotor modes: collective, backward (BW) and forward (FW) whirling. When using the Coleman approach, as it follows from [9, Equation (17)], each mode may contain up to three frequency components, the magnitude of all three blades are the same, and the phase lag of the *whirling components* will always be $\pm 120^0$.

In the presence of gravity, and/or when the rotor is anisotropic, the Floquet analysis needs to be applied. Figure 2 shows the Fourier components of the BW mode, its principal frequency is $\omega_{\mathrm{p}BW} \approx 0.48\,rad/s$. When the rotor is isotropic, with no gravity (Figure 2a), the mode consists of three components, (i) horizontal motion of the nacelle (x_C coordinate) at frequency $\omega_{\mathrm{p}BW} + 4\Omega \approx 4.50\,rad/s = 0.716Hz$, (ii) BW at $\omega_{\mathrm{p}BW} + 5\Omega \approx 5.51\,rad/s = 0.876Hz$ and (iii) FW at $\omega_{\mathrm{p}BW} + 3\Omega \approx 3.50\,rad/s = 0.556Hz$. The horizontal motion is superimposed by a much smaller vertical motion (y_C). The mode is called *backward whirling* since the rotor dynamic is dominated by this component. The FW component vanishes completely if the rotor support is symmetric, i.e., $k_V = k_H$.

Figure 2 also shows the complexity plots of the BW component. The phase lag between all three blades is the same, -120^0, and the amplitudes of the blades are also exactly equal.

As mentioned before, the same results could be obtained without Floquet analysis, by a much simpler Coleman transformation followed by eigenvalue decomposition of the system matrix **A** in (8), which is time-invariant in this case.

Due to gravity this mode gets enriched by more components, but only two are significant: those at $\omega_{\mathrm{p}BW} + 6\Omega \approx 6.51\,rad/s = 1.04Hz$ and $\omega_{\mathrm{p}BW} + 7\Omega \approx 7.52\,rad/s = 1.20Hz$, Figure 2b. As observed from the complexity plot, the blade amplitude is the same, so is the lag, -120^0.

Let's introduce a slight rotor anisotropy by reducing the stiffness of the third blade: k_3=0.99k. Due to this, a horizontal motion appears at $\omega_{\mathrm{p}BW} + 6\Omega \approx 6.51\,rad/s = 1.04Hz$, but its magnitude is significantly smaller than the main horizontal motion. More interesting, one can see that the blades' phase lag deviates now from -120^0. In addition, the amplitudes of different blades are not the same anymore.

This behaviour becomes more pronounced when the stiffness k_3 decreases more, Figure 2d. This phenomena was also observed when the mass of one of the blades was changing.

Figure 3 shows the Fourier components of the FW mode. For the isotropic rotor case, when no gravity is present, its principal frequency is $\omega_{\mathrm{p}FW} \approx -0.383\,rad/s$. The mode is dominated by the horizontal motion of the nacelle at frequency $\omega_{\mathrm{p}FW} + 7\Omega \approx 6.66\,rad/s = 1.06Hz$ and FW at

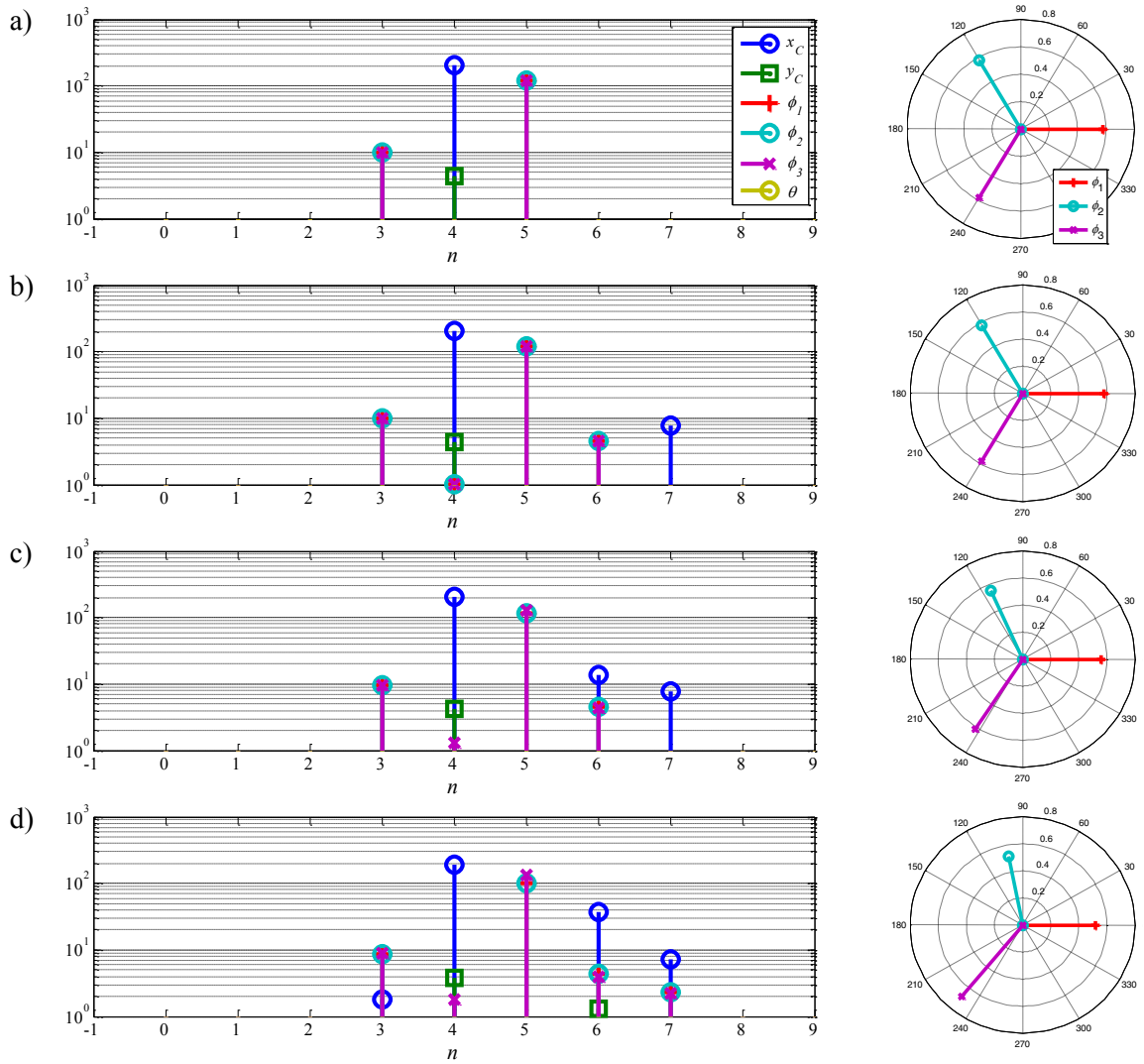

Figure 2: Backward whirling mode. Left: magnitude of Fourier components; right: complexity plot of the dominant whirling component n_{0BW}=4. a) Isotropic rotor, no gravity; b) isotropic rotor, with gravity; c) anisotropic rotor, k_c=0.99k; d) anisotropic rotor, k_c=0.97k.

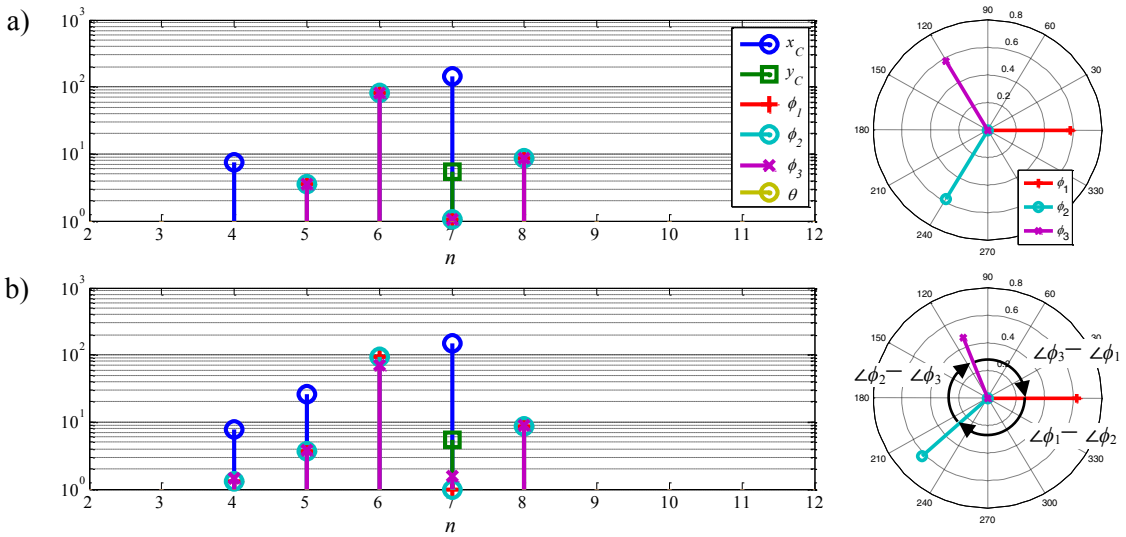

Figure 3: Forward whirling mode. Left: magnitude of Fourier components; right: complexity plot of the dominant whirling component n_{0FW}=7. a) Isotropic rotor, with gravity; b) anisotropic rotor, k_3=0.97k.

$\omega_{\mathrm{p}FW} + 6\Omega \approx 5.65\,rad/s = 0.899Hz$. The magnitude of the BW at $\omega_{\mathrm{p}FW} + 8\Omega \approx 7.66\,rad/s = 1.22Hz$ and the other components is significantly smaller. The mode is called *forward whirling* since the FW component dominates the rotor dynamics; the BW component is small and vanishes completely for the symmetric rotor support.

One may notice that the frequency of the dominating whirling components of the two considered modes are very close: 0.876 *Hz* and 0.899 *Hz*. This is not just a coincidence. This phenomenon can be explained by the close natural frequencies of the vertical and horizontal rotor modes when the rotor does not rotate, see e.g., the Campbell diagram [11, Figure 2]. If the stiffness values of the supporting structure are equal, k_V=k_H, one should expect the frequencies of the dominating whirling components of the two previously described modes to be exactly the same.

3 DAMAGE FEATURES

Based on the observations above, several modal-related damage features are suggested: (i) phase between the blades for the whirling component; (ii) amplitudes of the whirling component; (iii) amplitude of the non-dominant horizontal component. The sensitivity of these damage features are examined below.

The first suggested damage feature is based on the shape of the dominant whirling component of the two whirling modes. These Fourier components are n=5 for BW and n=6 for FW modes (see Figures 2, 3). Figure 4a shows how the phase lag depends on k_3. The calculation of the phase lag is visualized in Figure 3b, right. One per-cent reduction of k_3 causes the change of the phase lag between two undamaged blades by about 5-6% and 2-3% between damaged and undamaged blades.

All three blades have the same magnitude for isotropic rotors, but start to differ when the rotor becomes anisotropic, see Figure 4c,d for BW and FW modes respectively; the blades amplitude is normalized against the amplitude of the isotropic rotor. The damaged blade amplitude increases for the BW mode and decreases for the FW mode. The changes are about 4-6% for 1% reduction of k_3.

It is important to note that both features give the indication of which blade is damaged.

Non-dominant horizontal component also changes with increase of rotor anisotropy. This is the Fourier component n=6 for the BW mode and n=5 for the FW mode (Figure 2,3); it increases about 5-7% per 1% reduction of k_3. This damage feature does not indicate damage location. However, it does not require getting measurements from the blades and can be extracted from the nacelle acceleration measurements.

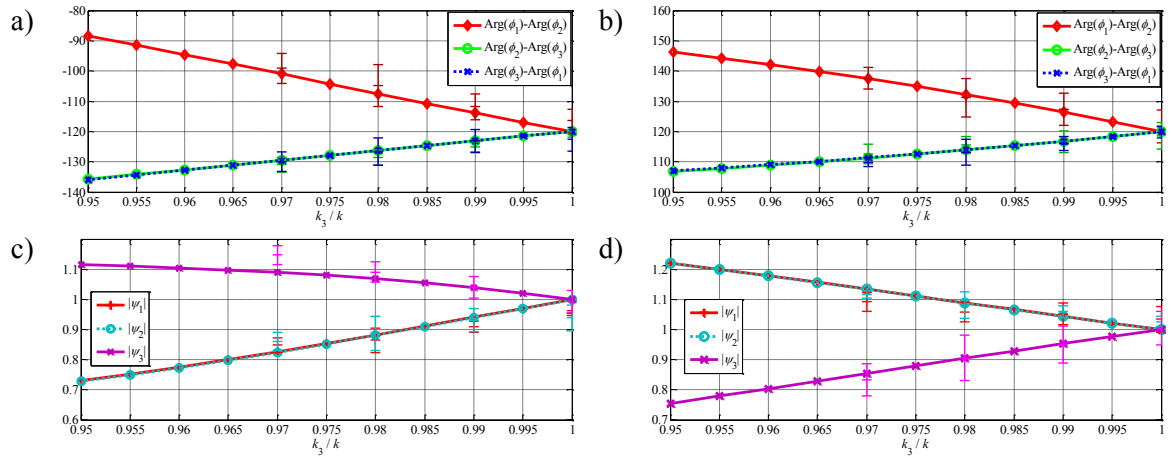

Figure 4: Damage features vs. stiffness k_3. a) phase lag BW mode; b) same, FW mode; c) normalized blades amplitudes, BW mode; d) same, FW mode.

For comparison, a one per-cent decrease of k_3 causes only 0.14-0.17% change of the natural frequencies. Therefore, these damage features used in typical SHM systems are more than 30 times less sensitive to damage than those described here.

4 OBSERVABILITY

The analytical study in the previous section was based on the known EoM. In this section, the same system is being studied from the experimental point of view, with the objective of finding out if the suggested damage features are derivable from experimental data.

In this section, we model a measurement system installed on the test object (Figure 1): accelerometers are attached to the tips of all blades, measuring in the tangential direction; two more accelerometers measure vertical and horizontal motion of the nacelle and an angular vibration accelerometer is installed on the drivetrain. All DOFs are excited by a random uncorrelated broadband noise. This excitation satisfies OMA assumptions but we acknowledge that the real aeroelastic forces are different [6]. Here the EoM is numerically integrated, and response time histories for the physical DOFs are obtained and converted to the signals that would be measured if the sensors were installed. From this point, we assume that the excitation forces and EoM are not known, so the damage features will be derived from the observed responses.

For the simulations, MATLAB's *ode45* routine was used, 7200 s long time histories corresponding to 1152 rotor revolutions were synthesized and sampled at 50 Hz. The time histories were used as an input to Brüel & Kjær Type 7760 OMA software. The modal analysis was performed by the Stochastic Subspace Iteration SSI algorithm. Four system states, one undamaged and three damaged (k_3=0.99, 0.98 and 0.97) were analysed. To collect statistics, five different load realisations were generated for each state, thus in total 20 analyses were performed.

Note the direct application of OMA to the data - neither Coleman transformation nor any other pre-processing were applied. Therefore, it was not expected to acquire the non-dominant components of the modes. In order to identify them, more sophisticated methods are required, e.g., the method based on Harmonic Power Spectra, either in frequency or time domain [5, 14].

The results of the simulated experiment are shown as error bars in Figure 4. The centre tick denotes the mean of the five OMA runs, the upper and lower ticks denote 95% confidence interval. The damage features derived from the OMA results are in agreement with analytical values - there is significant dispersion, especially for the magnitudes but the general tendency and the curves slope are correctly reflected, which is the most important for damage features of a SHM system.

5 CONCLUSION

Novel damage features for a potential SHM system of a wind turbine rotor are suggested and examined. The features are modal-based and utilise mode shape asymmetry due to rotor anisotropy caused by blade damage. It is demonstrated that these features are significantly more sensitive to the damage compared to the natural frequencies of the rotor. It was also shown that these features are observable in a real life scenario, i.e., they can be obtained by OMA performed on measured vibrations.

A simple 6 DOF analytical model of a rotating rotor was considered. Using Floquet analysis the exact modal decomposition was performed, and the sensitivities of the suggested damage features were numerically computed as a function of the damage size.

A simulated experiment confirmed that the damage features can be extracted from measured vibration responses using OMA.

ACKNOWLEDGEMENTS

The work is partly supported by EUDP (Danish Energy Technology Development and Demonstration Programme), grant number 64011-0084 “Predictive Structure Health monitoring of Wind Turbines”.

REFERENCES

[1] D. Montalvão, N.M.M. Maia, A.M.R. Ribeiro. A Review of Vibration-based Structural Health Monitoring with Special Emphasis on Composite Materials. *The Shock and Vibration Digest*, 38(4):295-324, July 2006.

[2] W. Fan, P. Qiao. Vibration-based Damage Identification Methods: A Review and Comparative Study. *Structural Health Monitoring*, 10(1):83-111, April 2010

[3] M.D. Ulriksen, D. Tcherniak, P.H. Kirkegaard, L. Damkilde. Operational Modal Analysis and Wavelet Transformation for Damage Identification in Wind Turbine Blades. *Proceedings of 7th European Workshop on Structural Health Monitoring*. Nantes, France, July 2014 (accepted for publication).

[4] D. Tcherniak, J. Basurko, O. Salgado, I. Urresti, S. Chauhan, C.E. Carcangiu, M. Rossetti. Application of OMA to operational wind turbine. *Proceedings of Int. Operational Modal Analysis Conference*. Istanbul, Turkey, May 2011.

[5] S. Yang, D. Tcherniak, M.S. Allen. Modal Analysis of Rotating Wind Turbine using Multiblade Coordinate Transformation and Harmonic Power Spectrum. *Proceedings of 32nd Int. Modal Analysis Conference*. Orlando, FL, USA, February 2014

[6] D. Tcherniak, S. Chauhan, M. H. Hansen. Applicability limits of Operational Modal Analysis to Operational wind turbines. *Proceedings of the 28th Int. Modal Analysis Conference (IMAC XXVIII)*. Jacksonville, FL, USA, February 2010.

[7] M.S. Allen, M.W. Sracic, S. Chauhan, M.H. Hansen, Output-Only Modal Analysis of Linear Time Periodic Systems with Application to Wind Turbine Simulation Data. *Mechanical Systems and Signal Processing*. 25:1174-1191, 2011.

[8] P.F. Skjoldan, M. H. Hansen. On the similarity of the Coleman and Lyapunov-Floquet transformations for modal analysis of bladed rotor structures. *Journal of Sound and Vibration*. 327:424-439, 2009.

[9] M.H. Hansen. Improved Modal Dynamics of Wind Turbines to Avoid Stall-induced Vibrations. *Wind Energy* 6:179-195, 2003.

[10] P.F. Skjoldan, O.A. Bauchau. Determination of Modal Parameters in Complex Nonlinear Systems. *Journal of Computational and Nonlinear Dynamics.* 6(3) 2011.

[11] M.H. Hansen. Aeroelastic Instability Problems for Wind Turbines, *Wind Energy.* 10: 551-577. 2007.

[12] P.F. Skjoldan. Aeroelastic Modal Dynamics of Wind Turbines Including Anisotropic Effects. *PhD Dissertation.* 2011.

[13] P.F. Skjoldan. Modal Dynamics of Wind Turbines with Anisotropic Effects. *47th AIAA Aerospace Sciences Meeting*. Orlando, FL, USA, January 2009.

[14] D. Tcherniak, M. Allen, S. Yang. Experimental characterization of operating wind turbine using Harmonic Power Spectra and Stochastic Subspace Identification. *Conference on Noise and Vibration Engineering (ISMA).* Leuven, Belgium. September 2014 (submitted).